

1 Background

Automated ultrasound using the Vega™ imager has been shown to be effective at noninvasively staging liver disease in many different rodent models, including:

- CCl4 [1] • Western Diet [3]
- Cholestasis [2] • Choline-Deficient Diet [4]

GOAL: To evaluate tracking response-to-therapy with automated ultrasound (US) in a preclinical study in a rodent models of MASH.

RATIONALE: Why use *in vivo* imaging for liver research?

1. *In vivo* imaging is non-disruptive to tissue, allowing a quick window into longitudinal disease progression within individual mice.
2. Diet-induced models require extended study durations, so timing endpoints is crucial to reduce waste and cost.
3. Can be used to remove outliers and reduce intra-group variability.

2 Imaging Methods

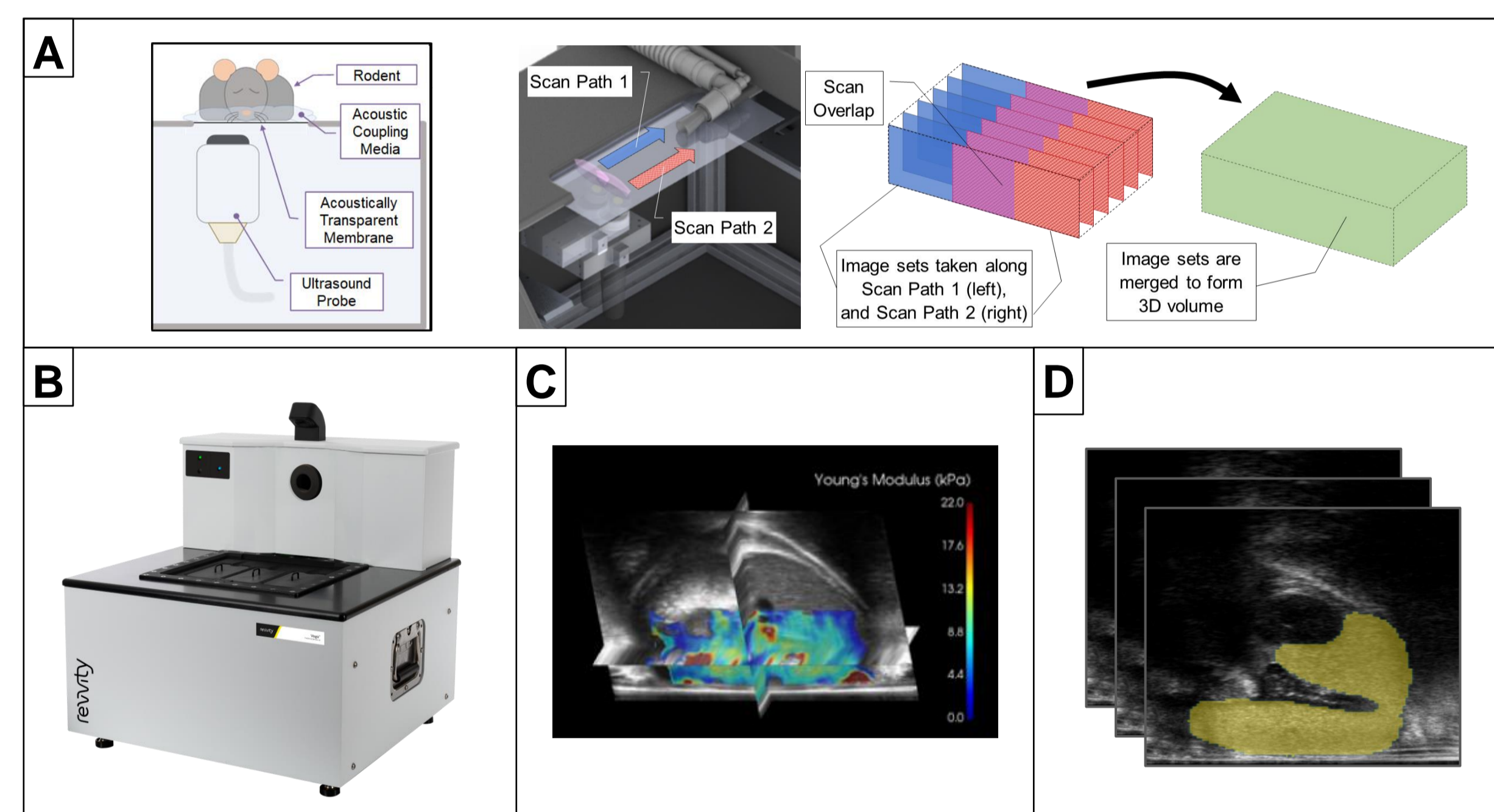


Figure 1: Schematic overview of image acquisition approach.

A: Rodents are placed on the ultrasound instrument in prone position and imaged from below via robotically controlled raster scan. Raw 2D frames are reconstructed into 3D volumes.

B: Photograph of Vega (Revvity, Inc.) ultrasound *in vivo* imaging system.

C: Screenshot of multi-modal 3D B-mode and Shear Wave Elastography scan of a mouse liver in orthoslice view.

D: Screenshot showing output of AI-assisted 3D liver segmentation (yellow outline). Segmentation is used to quantify liver volume.

3 Study Design

12-week-old C57Bl/6CrJ female mice were fed a choline-deficient high fat diet (N=16, "CDAHFD", A06071302, Research Diets). After 8 weeks, half of the mice (N=8) were switched to standard HFD (A06071306, Research Diets). A third control group (N=8) was fed standard chow. Imaging was performed every 2 weeks for 18 weeks.

Mice were imaged longitudinally with 3D ultrasound (described in Fig 1). Liver "echogenicity" (i.e. brightness) and liver stiffness were measured at each timepoint following manual segmentation of liver boundary. Liver volume was measured by AI-assisted segmentation for the entire longitudinal dataset, and manual segmentation for the final timepoint (18 wks).

At the final timepoint, prior to euthanasia, mice were imaged additionally with contrast-enhanced μ CT (Quantum GX2, Revvity). Fenestra HDVC (MediLumine) was injected 24h prior to imaging. Following euthanasia, livers were harvested, weighed, bisected, fixed in formalin, and shipped to RevealBio (CellCarta) for digital pathology analysis. Histological staining included H&E and Picrosirius Red (PSR), followed by automated quantification of steatosis, inflammation, and fibrosis from digitized slides.

4 Representative In Vivo Image Data

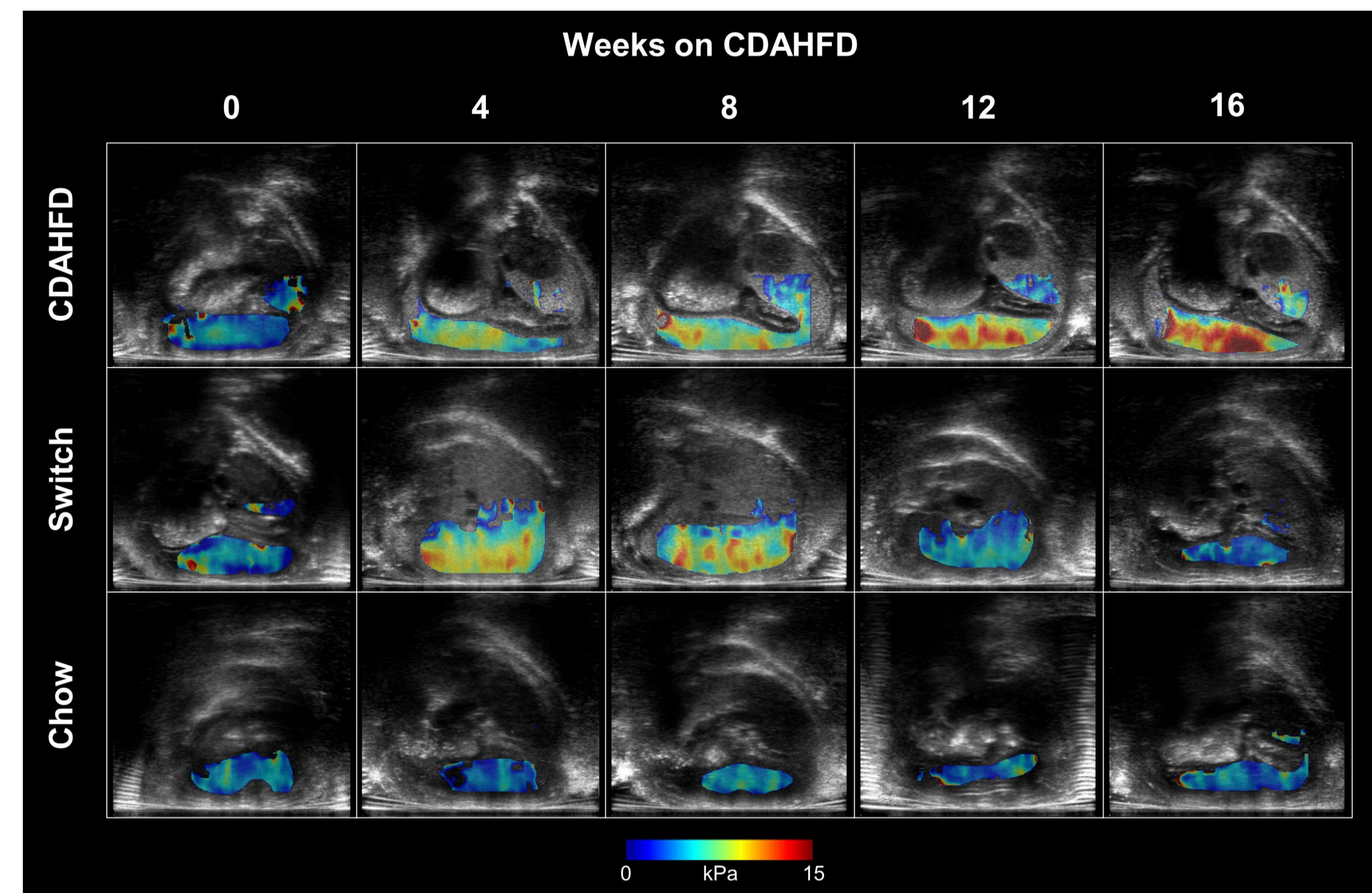


Figure 2: Representative longitudinal liver ultrasound images (axial plane) in the three different groups across the course of the CDAHFD diet-reversal study. Shear wave elastography (SWE) scans are overlaid on grayscale B-mode images. CDAHFD elicited a strong response in noninvasive markers of liver echogenicity, stiffness, and volume, with clear reversal at the diet switch timepoint (8 wks).

5 In Vivo Longitudinal Quantification

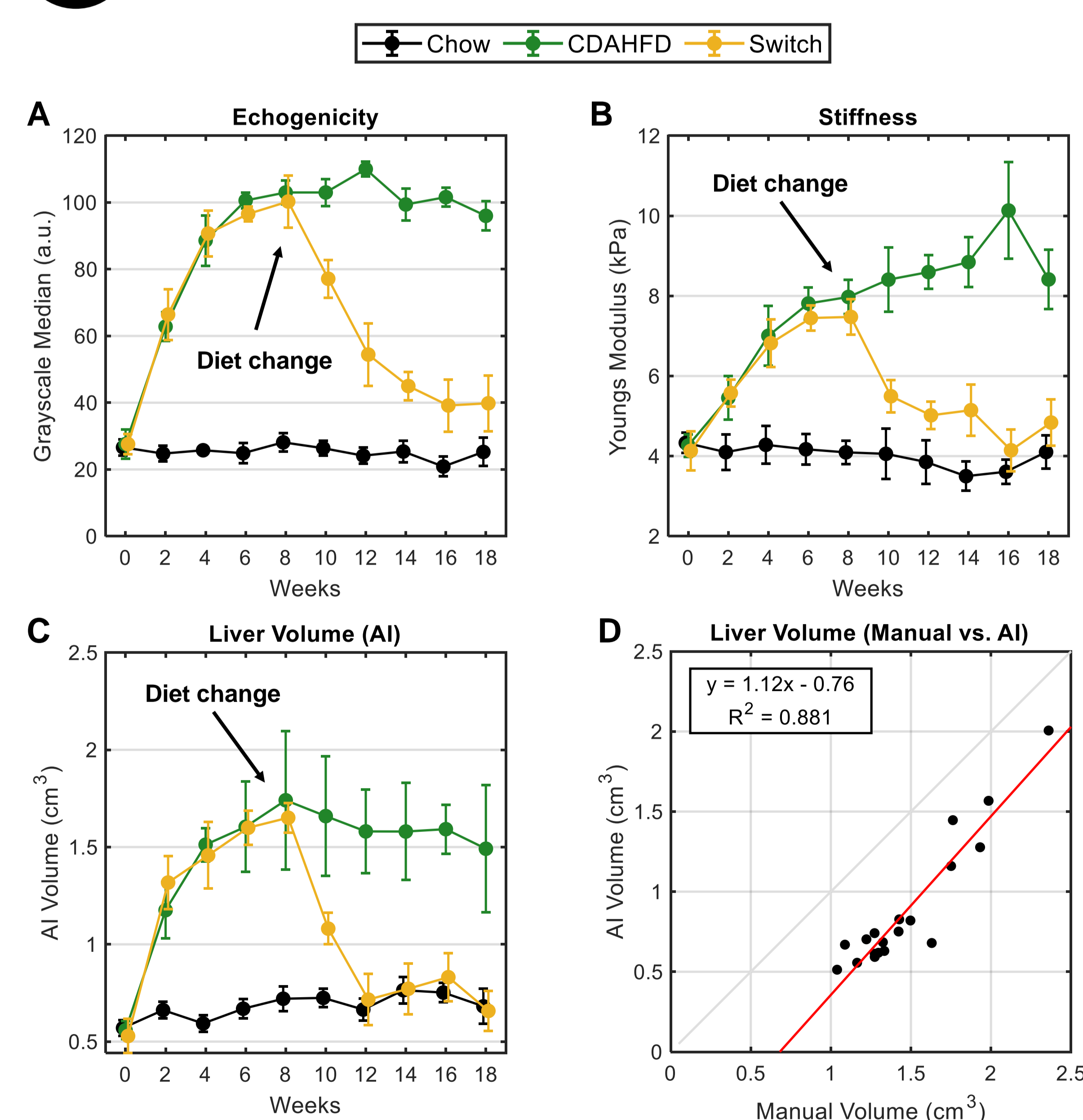


Figure 3: Longitudinal progression of liver echogenicity (A), stiffness (B), and liver volume (C) over 18 weeks in mice fed CDAHFD, standard chow, or switch from CDAHFD \rightarrow HFD chow. Error bars represent mean \pm std. Longitudinal liver volume plot (C) was generated using a fully automatic AI segmentation model. As seen by the linear regression plot (D) comparing a subset of AI-annotated and human-annotated images (18 wks timepoint), the AI model exhibits strong correlation to manual results, but with significant negative bias. Care must be taken when evaluating absolute measurements from AI.

6 Representative Histology Images

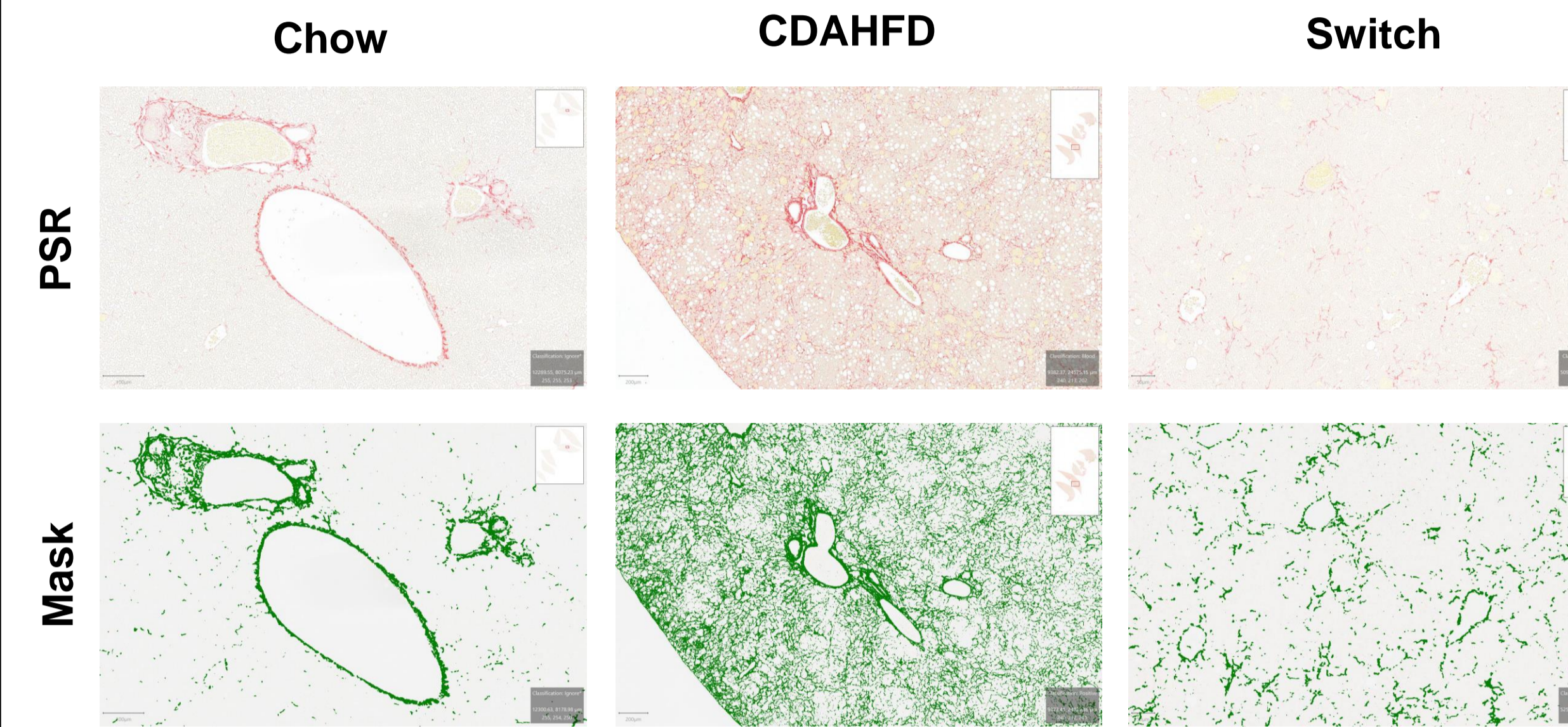


Figure 4: Representative histology images. Picrosirius red (PSR) stain is shown in top row, while the quantitation mask for % fibrosis area is shown in the bottom row (green pixels).

7 In Vivo Vs. Ex Vivo Comparison

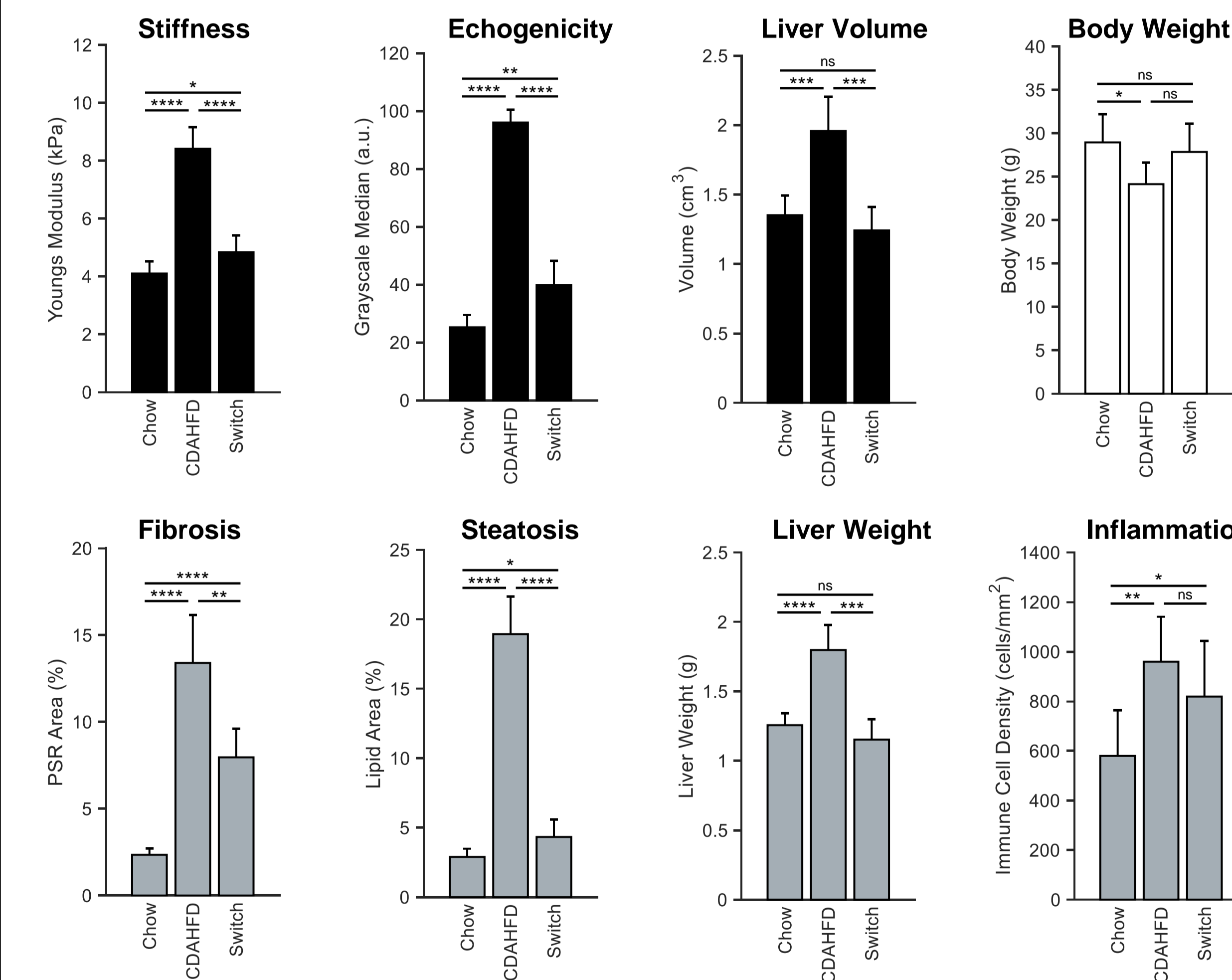


Figure 5: Comparison between *in vivo* imaging measurements and *ex vivo* measurements at 18-week timepoint. Note that liver volume for this timepoint was manually segmented by a human reader. * $p < 0.05$; ** $p < 0.01$; *** $p < 0.001$; **** $p < 0.0001$; ns, $p > 0.05$

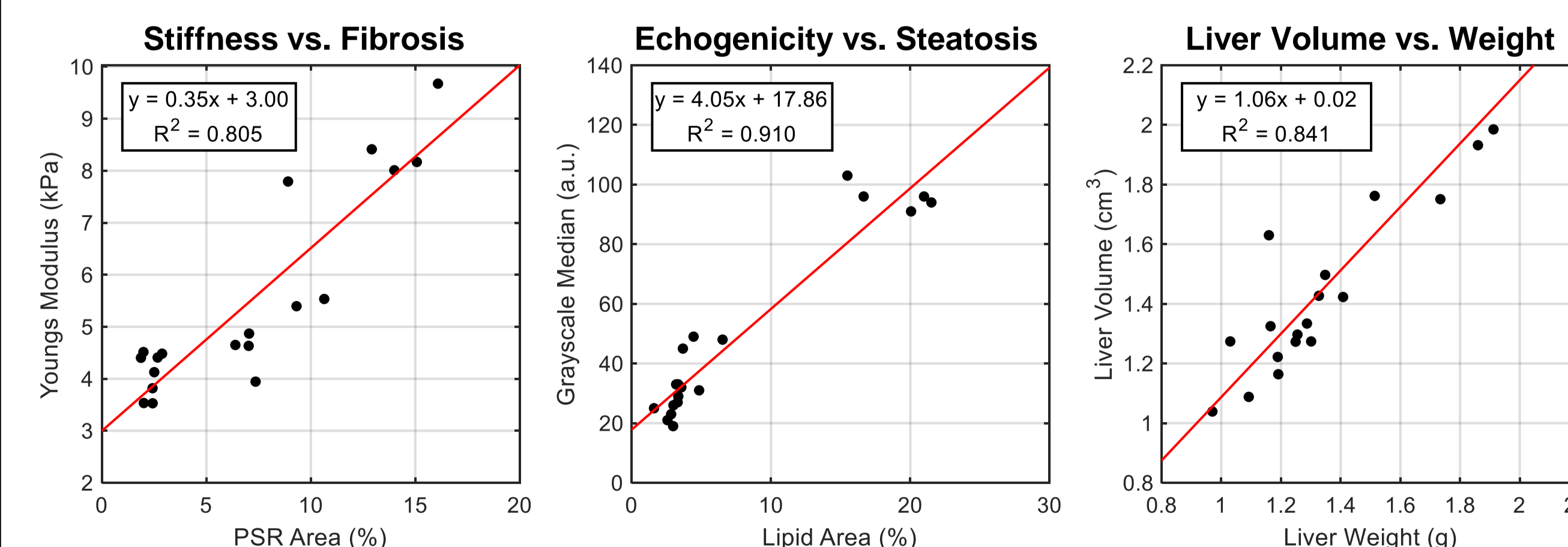


Figure 6: Linear regression analysis between *in vivo* imaging measurements and *ex vivo* measurements at 18-week timepoint. R^2 , coefficient of determination.

8 In Vivo Liver Volumetry: US vs. CT

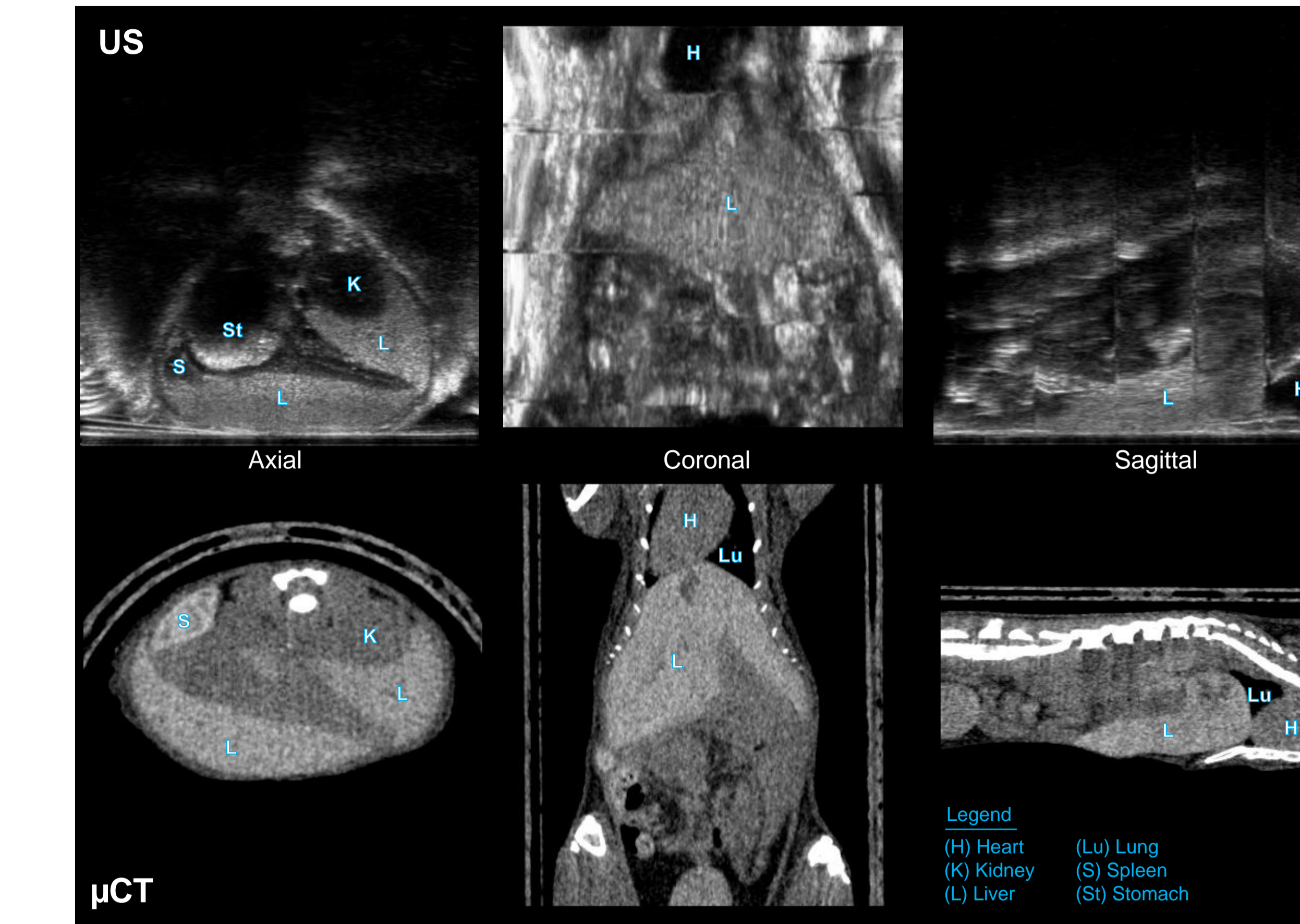


Figure 7: Comparison of *in vivo* liver volumetry performed by 3D US imaging and contrast-enhanced (CE) μ CT imaging. Although CE- μ CT offers superior resolution and is less prone to artifacts, strong agreement was observed between both modalities. Steatosis in the liver acts as an endogenous contrast enhancer in US, resulting in improved border definition.

9 Conclusions

These studies demonstrate the potential of an automated robotic ultrasound system to provide noninvasive insights into the progression (and regression) of critical phenotypes with strong correlation to histological ground truth and gold-standard contrast-enhanced *in vivo* imaging. 3D US with Vega was fast, typically <5 min per animal, but required a serial subject workflow. Further enhancements made to the data acquisition instrument, such as real-time SWE, can further reduce scanning time and enable parallelized subject data capture.

In this work, we also demonstrated for the first time fully automated AI-assisted liver volumetry in a practical manner. While AI-predicted liver volumes underestimated ground truth and human segmented volumes, the longitudinal trends followed the expected disease progression time course exceptionally well. We expect future iterations of the AI model to improve in both accuracy and bias as the training data sets increase in size and breadth.

Funding sources: NIH SB1DK112492